

Ruthenium(II) Pyridylimidazole Complexes as Photoreductants and PCET Reagents

Andrea Pannwitz,^[a] Alessandro Prescimone,^[a] and Oliver S. Wenger^{*[a]}

Abstract: Complexes of the type $[\text{Ru}(\text{bpy})_2\text{pyimH}]^{2+}$ (bpy = 2,2'-bipyridine, pyimH = 2-(2-pyridyl)imidazole) with various substituents on the bpy ligands can act as photoreductants. Their reducing power in the ground state and in the long-lived $^3\text{MLCT}$ excited state is increased significantly upon deprotonation, and they can undergo proton-coupled electron transfer (PCET) in the ground and excited state. PCET with proton and electron originating from a single donor resembles hydrogen atom transfer (HAT) and can be described thermodynamically by formal bond dissociation free energies (BDFEs). While the class of complexes studied herein has long been known, their N-H BDFEs have never been determined even though this is important in view of assessing their reactivity. Our study demonstrates that the N-H BDFEs in the $^3\text{MLCT}$ excited states are between 34 kcal mol^{-1} to 52 kcal mol^{-1} depending on the chemical substituents at the bpy spectator ligands. Specifically, we report on the electrochemistry and PCET thermochemistry of three heteroleptic complexes in 1:1 (v:v) $\text{CH}_3\text{CN} / \text{H}_2\text{O}$ with CF_3 , $t\text{Bu}$ and NMe_2 substituents on the bpy ligands.

input.^[9–13] In some previous studies, photons were used to generate reactive species which could subsequently undergo PCET in the electronic ground state.^[14–19] A very promising approach is the use of photoexcited metal complexes and external bases or acids.^[10,11,20,21] PCET reactions and even hydride transfer directly involving the excited state species are possible and have received increasing attention.^[22–32]

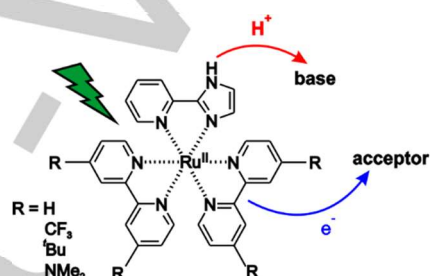


Figure 1. Investigated $[\text{Ru}^{\text{R}}\text{pyimH}]^{2+}$ complexes and their PCET reactivity.

Introduction

In the context of photochemistry and solar energy conversion, transition metal complexes traditionally play an important role. Especially d^6 metal complexes such as $\text{Ru}(\text{bpy})_3^{2+}$ are useful photosensitizers, due to long-living $^3\text{MLCT}$ excited states which are accessible with visible light irradiation.^[1,2] Redox processes from this state are energetically favored compared to the ground state, and absorbed light energy can be transformed into chemical energy, for example by photoredox catalysis in organic synthesis,^[3–5] or the generation of so-called solar fuels.^[6–8] In the general context of redox catalysis and charge transfer, the coupling to proton transfer can play a crucial role because energy barriers can be lowered substantially by proton-coupled electron transfer (PCET), and reduction products can be stabilized by protonation whereas oxidation products can be stabilized by deprotonation. It would be attractive to combine the benefits of PCET with the principle of using light as the principal energy

We report here on the ground and excited state properties of a family of ruthenium diimine complexes bearing a pyimH ligand (Figure 1). The imidazole unit of the pyimH ligand can be deprotonated, and this drastically influences the redox properties of the entire complex. Strong reductants are accessible by photoexcitation, particularly when combined with deprotonation. Recently, we reported on the $[\text{Ru}^{\text{R}}\text{pyimH}]^{2+}$ complex with $\text{R} = \text{H}$, in which two unsubstituted bpy spectator ligands were present.^[27] Building on prior work,^[33,34] we demonstrated that the combined release of an electron and a proton makes this complex a very strong (formal) hydrogen atom donor in the long-lived $^3\text{MLCT}$ excited state. Mechanistically, formal hydrogen atom transfer (HAT) is a PCET process, but thermodynamically the determination of a formal N-H BDFE is meaningful.^[35,36] For the $[\text{Ru}^{\text{R}}\text{pyimH}]^{2+}$ complex with $\text{R} = \text{H}$ we determined 43 kcal mol^{-1} in 1:1 (v:v) $\text{CH}_3\text{CN} / \text{H}_2\text{O}$. In this work, we explored to what extent the formal N-H BDFE is tunable by altering the bpy spectator ligands. This seems important in view of tailoring the excited-state redox and PCET reactivity for specific applications.

In general, the BDFE for an X-H bond can be estimated from the reaction free energies associated with the individual electron and proton transfer steps as shown in the so-called square scheme in Scheme 1. Proton transfer (PT) and electron transfer (ET) are thermodynamically characterized by the acidity constant (pK_a) and the redox potential (E°), respectively. In aqueous solution, the N-H BDFE can be calculated with equation 1 where E° must be entered in units of V vs. NHE, and the last summand is a solvent

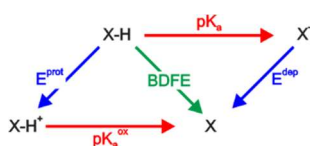
[a] A. Pannwitz, A. Prescimone, O. S. Wenger
Department of Chemistry
University of Basel
St. Johanns-Ring 19 and Spitalstrasse 51, CH-4056 Basel,
Switzerland
E-mail: oliver.wenger@unibas.ch
Homepage: www.chemie.unibas.ch/~wenger/index.html

Supporting information for this article is given via a link at the end of the document.

FULL PAPER

characteristic parameter describing solvation of hydrogen atoms.^[35]

$$\text{BDFE (N-H)} = 1.37 \text{ p}K_{\text{a}} + 23.06 \text{ E}^{\circ} + 57.6 \text{ kcal mol}^{-1} \quad (\text{eq. 1})$$



Scheme 1. Thermochemical square scheme for the cleavage of X-H bonds by individual deprotonation ($\text{p}K_{\text{a}}$, $\text{p}K_{\text{a}}^{\text{ox}}$) and oxidation steps (E^{prot} , E^{dep}).

As noted above, the complex with $\text{R} = \text{H}$ exhibits a formal N-H BDFE of only 43 kcal mol^{-1} ,^[27] which is comparable to metal hydride complexes such as $\text{HV}(\text{CO})_4(\text{P-P})$ (with $\text{P-P} = \text{Ph}_2\text{P}(\text{CH}_2)_n\text{PPh}_2$) or $(\text{Cp})\text{Cr}(\text{CO})_3\text{H}$ (with $\text{Cp} = \text{cyclopentadienyl}$). The low N-H BDFE in our $[\text{Ru}^{\text{H}}\text{pymH}]^{2+}$ complex results from the conversion of light energy into chemical energy, and it manifests by the lowering of the N-H BDFE by $\sim 50 \text{ kcal mol}^{-1}$ between the ground and the excited state. This energy difference corresponds essentially to the absorbed visible photon. In this work, three derivatives of the parent complex with different chemical substituents at the 4- and 4'-positions of the bpy spectator ligands are characterized in their ground and excited states in 1:1 (v:v) $\text{CH}_3\text{CN} / \text{H}_2\text{O}$ mixture. We find that it is possible to tune the excited-state BDFEs between 52 kcal mol^{-1} ($\text{R} = \text{CF}_3$) and 34 kcal mol^{-1} ($\text{R} = \text{NMe}_2$), the latter being an unusually low value.^[10,37,38]

Results and Discussion

Synthesis and Crystallographic Characterization

All commercially available chemicals for synthesis, including 4,4'-di-*tert*-butyl-2,2'-bipyridine and $\text{RuCl}_3 \cdot 3 \text{H}_2\text{O}$, were used as received. The syntheses of the ligands 2-(2-pyridyl)imidazole (pymH) and 4,4'-bis(dimethylamino)-2,2'-bipyridine followed known procedures.^[39,40] All $[\text{Ru}^{\text{R}}\text{pymH}]^{2+}$ complexes were isolated as PF_6^- salts. The preparation of $[\text{Ru}^{\text{CF}_3}\text{pymH}](\text{PF}_6)_2$ followed the previously published procedure.^[41] The syntheses of $[\text{Ru}^{\text{tBu}}\text{pymH}](\text{PF}_6)_2$ and $[\text{Ru}^{\text{NMe}_2}\text{pymH}](\text{PF}_6)_2$ were similar.^[40–42] Synthetic procedures, including complex and ligand syntheses are reported in the experimental section and supporting information.

Monocrystalline needles of $[\text{Ru}^{\text{NMe}_2}\text{pymH}](\text{PF}_6)_2$ were obtained by slow diffusion of diethyl ether into a solution of the compound in acetonitrile. It crystallized in space group $P\bar{1}$ with two PF_6^- counter ions, 0.5 acetonitrile and 0.5 diethyl ether molecules per complex in the asymmetric unit. Crystallographic details are included in the supporting information and CCDC-1518357 contains the supplementary crystallographic data for this paper. These data can be obtained free of charge from The Cambridge Crystallographic Data Centre via www.ccdc.cam.ac.uk/data_request/cif.

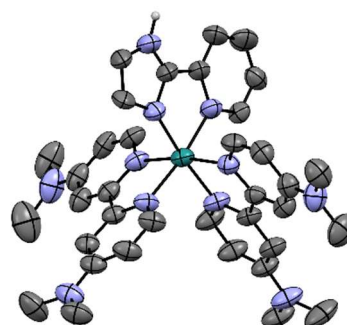


Figure 2. Crystal structure of $[\text{Ru}^{\text{NMe}_2}\text{pymH}]^{2+}$. Thermal ellipsoids are drawn at the 50 % probability level. Solvent molecules, counter ions and hydrogen atoms, except N-H, are omitted for clarity.

Redox and Acid-Base Chemistry

As described in the introduction, the formal BDFE of the pymH N-H functionality can be calculated on the basis of redox and acid-base properties to predict formal HAT or PCET behavior in the ground and excited states.^[27,35] For the $[\text{Ru}^{\text{R}}\text{pymH}]^{2+}$ complexes with $\text{R} = \text{CF}_3$, tBu and NMe_2 , the relevant parameters were determined analogously to our previously published example of $[\text{Ru}^{\text{H}}\text{pymH}]^{2+}$.^[27] For the determination of the ground state acidity constant ($\text{p}K_{\text{a}}$), the spectral changes occurring in the spectral range of the $^1\text{MLCT}$ absorption band were monitored as a function of pH (supporting information Figures S1 - S3). Pourbaix diagrams (Figure 3) were established on the basis of cyclic voltammograms recorded at different pH values (supporting information Figures S4 - S6). There are three different regimes: At very basic pH, the redox potential E^{dep} is pH-independent because the complex is deprotonated in both the Ru^{II} and Ru^{III} oxidation states. The redox potential in the strongly acidic pH regime, E^{prot} , is also pH-independent because the complex is protonated irrespective of whether the oxidation state is +II or +III. In the intermediate pH regime, the redox potential is expected to shift with a slope of $-59 \text{ mV per pH unit}$. For $\text{R} = \text{tBu}$ and NMe_2 , the oxidation process is reversible and the slopes in the one-electron-one-proton regime are -52 mV pH^{-1} and -54 mV pH^{-1} respectively (Figure 3b/c). For $\text{R} = \text{CF}_3$, a slope of -74 mV pH^{-1} was determined (Figure 3a). This deviation from ideal behavior is attributed to the irreversible nature of the one-electron oxidation process in this specific complex. In all three complexes, the acidity constant decreases by 4 to 5 logarithmic units upon oxidation. $[\text{Ru}^{\text{CF}_3}\text{pymH}]^{2+}$ is the most acidic ($\text{p}K_{\text{a}} 7.2$) and $[\text{Ru}^{\text{NMe}_2}\text{pymH}]^{2+}$ is the least acidic complex due to the electronic influence of the substituents on the bpy spectator ligands (Table 1). The oxidation potential of all four pymH complexes shifts cathodically by ca. 0.3 V upon deprotonation, in line with prior reports on iron and ruthenium complexes with deprotonatable ligands.^[43–46] The highest oxidation potential is observed with the CF_3 -substituents ($\text{E}^{\text{prot}} = 1.28 \pm 0.05 \text{ V vs. SCE}$ for the protonated and $\text{E}^{\text{dep}} = 0.98 \pm 0.05 \text{ V vs. SCE}$ for the deprotonated complex, respectively). The lowest oxidation potential is detected for the complex with NMe_2 -substituents ($\text{E}^{\text{prot}} = 0.41 \pm 0.05 \text{ V}$ and $\text{E}^{\text{dep}} = 0.17 \pm 0.05 \text{ V vs. SCE}$, respectively).

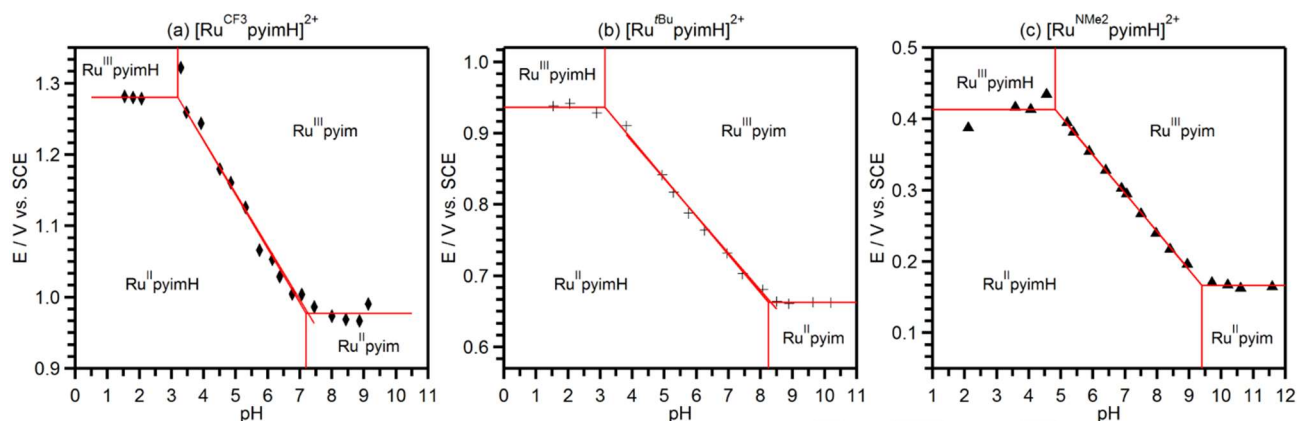


Figure 3. Pourbaix diagrams for $[\text{Ru}^{\text{R}}\text{pyimH}]^{2+}$ in 1:1 (v:v) $\text{CH}_3\text{CN} / \text{H}_2\text{O}$ with 0.05 M buffer. The slopes for the one-electron one-proton redox processes are (a) -74 mV pH^{-1} , (b) -52 mV pH^{-1} , (b) -54 mV pH^{-1} , established based on the cyclic voltammetry data shown in Figures S4 – S6 of the supporting information.

Table 1. Thermodynamic parameters for the $[\text{Ru}^{\text{R}}\text{pyimH}]^{2+}$ complexes in 1:1 (v:v) $\text{CH}_3\text{CN} / \text{H}_2\text{O}$: Acidity constants in the electronic ground state (pK_a), in the long-lived $^3\text{MLCT}$ excited state (pK_a^*) and in the one-electron oxidized form (pK_a^{ox}), oxidation potential in the ground state, $^3\text{MLCT}$ energy and oxidation potential in the excited state for protonated complex (E^{prot} , E_{00}^{prot} , $^*E^{\text{prot}}$) and deprotonated complex (E^{dep} , E_{00}^{dep} , $^*E^{\text{dep}}$).

R	pK_a	pK_a^*	pK_a^{ox}	E^{prot} [V vs. SCE]	E_{00}^{prot} [eV] [a]	$^*E^{\text{prot}}$ [V vs. SCE]	E^{dep} [V vs. SCE]	E_{00}^{dep} [eV] [a]	$^*E^{\text{dep}}$ [V vs. SCE]
H [b]	8.1 ± 0.1	5.6 ± 0.3	3.6 ± 0.1	1.00 ± 0.05	2.1 ± 0.1	-1.1 ± 0.1	0.73 ± 0.05	1.9 ± 0.1	-1.2 ± 0.1
CF_3	7.2 ± 0.1	5.3 ± 1 [c]	3.2 ± 0.1	1.28 ± 0.05	1.9 ± 0.1	-0.6 ± 0.1	0.98 ± 0.05	1.8 ± 0.1	-0.8 ± 0.1
^tBu	8.2 ± 0.1	5.4 ± 0.3	3.2 ± 0.1	0.94 ± 0.05	2.1 ± 0.1	-1.1 ± 0.1	0.66 ± 0.05	2.0 ± 0.1	-1.3 ± 0.1
NMe_2	9.2 ± 0.1	8.4 ± 0.5	4.8 ± 0.1	0.41 ± 0.05	2.0 ± 0.1	-1.6 ± 0.1	0.17 ± 0.05	1.9 ± 0.1	-1.7 ± 0.1

[a] from luminescence spectra recorded at 77 K in ethanol / methanol mixture, shown in the supporting information. [b] from reference [27]. [c] from reference [41].

Excited state oxidation potentials ($^*E^{\text{prot}}$, $^*E^{\text{dep}}$) were estimated with eq. 2 and eq. 3 based on the relevant ground state oxidation potentials (E^{prot} , E^{dep}). $^3\text{MLCT}$ energies were determined at 77 K for the protonated (E_{00}^{prot}) and deprotonated complexes (E_{00}^{dep}) (supporting information Figure S7).

$$^*E^{\text{prot}} = E^{\text{prot}} - E_{00}^{\text{prot}} \quad (\text{eq. 2})$$

$$^*E^{\text{dep}} = E^{\text{dep}} - E_{00}^{\text{dep}} \quad (\text{eq. 3})$$

Photoacid Behavior and Excited-State Lifetimes

The acidity constant of the $^3\text{MLCT}$ state (pK_a^*) was estimated with the Förster equation based on the luminescence maxima of protonated and deprotonated complex (λ^{prot} , λ^{dep}) at room temperature in 1:1 (v:v) $\text{CH}_3\text{CN} / \text{H}_2\text{O}$.^[47] For R = H and CF_3 the pK_a^* values were already known,^[27,41] and for the complexes with R = ^tBu and NMe_2 the Förster method was applied. The resulting pK_a^* values were verified by pH-titration monitoring steady-state emission as shown in the supporting information in Figures S8 – S9. Because the π^* orbitals of the bpy ligands are energetically

lower-lying than the π^* orbitals of the pyimH ligand, electron density is withdrawn from the acidic N-H functionality and its acidity is increased in the emissive $^3\text{MLCT}$ states of all four complexes (Table 1) analog to other photoacids.^[34,48] Excited state acid-base equilibration takes place in the pH range between pK_a and pK_a^* , where the excited $[\text{Ru}^{\text{R}}\text{pyimH}]^{2+}$ complexes are deprotonated by solvent or buffer molecules. Proton release then very quickly leads to the deprotonated ground state. This can unambiguously be seen in the transient absorption spectra, which are essentially the difference between the UV-Vis spectra recorded before and after laser excitation (for R = ^tBu in Figure 4). At pH 3 (Figure 4a) and at pH 10 (Figure 4b), a bleach between 400 nm and 550 nm is detected, which originates from disappearance of the $^1\text{MLCT}$ absorption. Under basic conditions the bleach is red shifted, because the ground state is deprotonated and the $^1\text{MLCT}$ absorption band is red shifted compared to the protonated form. At pH 6 (Figure 4c), a positive signal at around 500 nm becomes detectable, which can be explained by deprotonation in the excited state and rapid

relaxation into the deprotonated ground state. When subtracting the UV-Vis spectrum of the $[\text{Ru}^{\text{tBu}}\text{pyimH}]^{2+}$ complex from that of its deprotonated congener, the spectrum in Figure 4d is obtained. This spectrum is very similar to the transient absorption spectrum in Figure 4c, from which we conclude that in the time-resolved laser experiment, the deprotonated complex in the ground state indeed accumulates. This effect is less pronounced for the complex with $\text{R} = \text{NMe}_2$, in which case the deprotonated ground state can only be detected after the excited state has completely decayed (supporting information Figure S11). Presumably, this is due to the weaker driving-force for proton release in this case and different complex - buffer interactions. The excited state lifetimes are shortened by 50 – 90 % upon deprotonation (Table 2), ranging from 70 to 210 ns for the protonated forms and from 17 to 75 ns for the deprotonated forms, respectively, in the absence of oxygen. This effect can be explained by the energy-gap law and by mixing of pyim⁻ based orbitals with metal centered d-orbitals. As a consequence, the resulting excited state in the deprotonated complexes has a non-negligible ligand-to-ligand charge transfer character, and this can contribute to the lifetime shortening relative to the protonated complex.^[34] The excited-state lifetimes under aerated conditions are reported in the supporting information in Table S3.

Table 2. Excited state properties of $[\text{Ru}^{\text{R}}\text{pyimH}]^{2+}$ at 25 °C in 1:1 (v:v) $\text{CH}_3\text{CN} / \text{H}_2\text{O}$ at: luminescence maxima protonated and deprotonated complexes (λ^{prot} , λ^{dep}) and lifetimes of protonated and deprotonated complexes (τ^{prot} , τ^{dep}) under deaerated conditions.

R	λ^{prot} [nm]	λ^{dep} [nm]	τ^{prot} [ns]	τ^{dep} [ns]
H ^[b]	625	675	210 ± 20	70 ± 7
CF ₃ ^[c]	670	708	160 ± 16	17 ± 5
^t Bu	625	683	140 ± 14	75 ± 8
NMe ₂	675	692	70 ± 7	25 ± 2

[b] taken from reference [27]. [c] taken from reference [41].

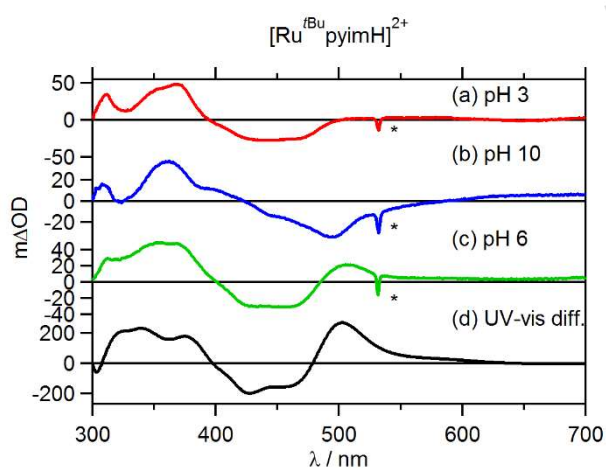


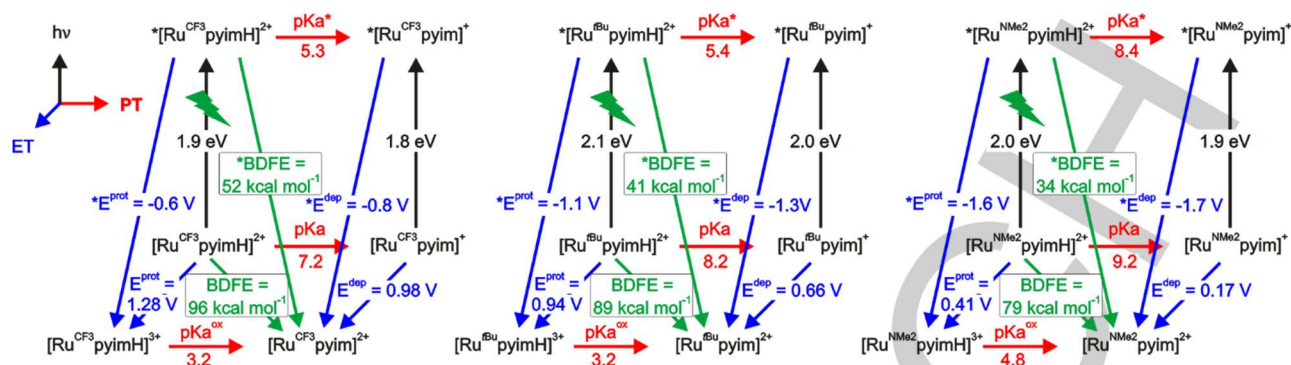
Figure 4. (a-c) Transient absorption spectra of $[\text{Ru}^{\text{tBu}}\text{pyimH}]^{2+}$ in 1:1 (v:v) $\text{CH}_3\text{CN} / \text{H}_2\text{O}$ at different pH values. Excitation occurred at 532 nm with laser pulses of ca. 10 ns duration, the spectra were recorded without time delay over

a period of 200 ns. (d) Difference of ground state UV-vis spectra of protonated and deprotonated complex. The asterisks mark laser stray light.

Formal N-H BDFEs

Based on the acidity constants and redox potentials in Table 1, formal N-H BDFEs were calculated with equation 1. The results are listed in Table 3. The values obtained for the ground state were doubly determined by using pK_a and E^{dep} on the one hand, and pK_a^{ox} and E^{prot} on the other hand. Both sets of data were measured independently of each other, and ultimately they lead to an internally consistent picture. The BDFEs for the electronic excited states (^{*}BDFE) were also doubly determined by using pK_a^* and E^{dep} , and by using pK_a^{ox} and E^{prot} , respectively. The double determinations yielded the same BDFEs within experimental accuracy. The general observation is that for every complex the N-H bond cleavage is facilitated by ~ 50 kcal mol⁻¹ in the excited state. The ground state BDFEs are in the range from 79 ± 1 kcal mol⁻¹ ($\text{R} = \text{NMe}_2$) to 96 ± 1 kcal mol⁻¹ ($\text{R} = \text{CF}_3$) which is comparable in magnitude to the N-H BDFEs of primary and secondary amines.^[35,49,50] Consequently, the BDFE can be tuned over a range of ~ 20 kcal mol⁻¹ by substituent variation at the bpy spectator ligands. The complete thermochemistry regarding proton and electron transfer in ground and excited states is summarized in Scheme 2 in so-called “cube”-schemes. In this representation, the ground state redox potentials for the protonated and deprotonated complexes are found on the bottom along with the acidity constants of the Ru^{II} and Ru^{III} species (pK_a and pK_a^{ox}). The bottom of Scheme 2 is in fact analogous to the thermodynamic square scheme for the cleavage of X-H bonds shown in Scheme 1. In Scheme 2, excitation to the ³MLCT state is represented by vertical arrows for both the protonated (E_{00}^{prot}) and deprotonated (E_{00}^{dep}) forms. In the excited state, the thermodynamically relevant processes are acid-base equilibration (pK_a^*) (marked by a horizontal red arrow) and oxidation of the ^{*}Ru^{II} complexes to give the respective Ru^{III} complexes in the electronic ground state, as represented by blue face diagonals (E^{prot} , E^{dep}). The combined loss of a proton and an electron from the excited state is shown on the space diagonal from the back upper left corner to the lower front right corner, indicated by ^{*}BDFE (green arrows).

Thus, for the excited state of $[\text{Ru}^{\text{NMe}_2}\text{pyimH}]^{2+}$ an exceptionally low ^{*}BDFE of 34 ± 5 kcal mol⁻¹ is found, and this is caused by the strongly electron donating NMe₂-groups which lead to a low potential for metal oxidation. The inverse effect accounts for the behavior of $[\text{Ru}^{\text{CF}_3}\text{pyimH}]^{2+}$, which has a relatively high ^{*}BDFE of 52 ± 5 kcal mol⁻¹. Nevertheless, even this ^{*}BDFE value is still on the order of magnitude reported for M-H cleavage in metal hydride catalysts that are used for thermal hydrogenation reactions.^[37,51] In summary, the N-H BDFEs in $[\text{Ru}^{\text{R}}\text{pyimH}]^{2+}$ complexes decrease with more electron donating substituents on the bpy spectator ligands. A similar finding was reported for the *ground-state* N-H BDFEs of ruthenium(II) 2-(2-pyridyl)imidazole complexes when going from hexafluoro-acetylacetonato (hfacac) to acetylacetonato (acac) spectator ligands which lead to a decrease of 80 to 62 kcal mol⁻¹.^[52]



Scheme 2 Thermodynamic “cube” scheme for $[\text{Ru}^{\text{R}}\text{pyimH}]^{2+}$ in 1:1 (v:v) $\text{CH}_3\text{CN} / \text{H}_2\text{O}$ based on the data in Tables 1 and 2. Horizontal / red: pK_a values, vertical / black: ${}^3\text{MLCT}$ energy E_{00} , pointing towards the reader in blue: oxidation potentials in V vs. SCE, diagonal in green: BDFEs.

Table 3 X-H Bond dissociation free energies in the ground (BDFE) and excited state (*BDFE) for some selected metal complexes which can be considered formal H-atom donors.

complex	BDFE [kcal mol ⁻¹]	*BDFE [kcal mol ⁻¹]	reference	comments
$[\text{Ru}^{\text{H}}\text{pyimH}]^{2+}$	91 ± 1	43 ± 5	[27]	
$[\text{Ru}^{\text{CF}_3}\text{pyimH}]^{2+}$	96 ± 1	52 ± 5	this work	
$[\text{Ru}^{\text{tBu}}\text{pyimH}]^{2+}$	89 ± 1	41 ± 5	this work	
$[\text{Ru}^{\text{NMe}_2}\text{pyimH}]^{2+}$	79 ± 1	34 ± 5	this work	
$[\text{Ru}(\text{bpy})_2\text{BiBzimH}_2]^{2+}$	90	42	[33,53,54]	[a, b]
$[\text{Ru}(\text{bpy})_2\text{BiimH}_2]^{2+}$	86	40	[33,53,54]	[a, b]
$[\text{Os}(\text{bpy})_2\text{BiBzimH}_2]^{2+}$	80	42	[33,53,54]	[a, b, c, e]
$[\text{Ru}(\text{hfacac})_2\text{pyimH}]^{2+}$	80	-	[55]	
$[\text{Ru}(\text{bpy})((\text{OH})_2\text{-phen})_2]^{2+}$	78	30	[56]	[a, b, d, f]

[a] BDFE calculated based on available redox potentials and acidity constants using both pathways illustrated in Scheme 1. [b] Excited-state bond dissociation free energies (*BDFEs) calculated based on available pK_a^{ox} , E^{prot} values. [c] Redox potentials only in CH_3CN available; [d] pK_a^{ox} determined via Nernst equation; [e] $E_{00} = 1.66$ eV, approximated from $[\text{Os}(\text{bpy})_3]^{2+}$, as reported in reference [57]; [f] $E_{00} = 2.1$ eV approximated from $[\text{Ru}(\text{bpy})_3]^{2+}$.^[58]

The strong decrease of the N-H BDFEs upon photoexcitation to values below 60 kcal mol⁻¹ is in line with our prior report on the $[\text{Ru}^{\text{R}}\text{pyimH}]^{2+}$ complex with $\text{R} = \text{H}$.^[27] In principle, this effect is also expected for other metal complexes that can release both a proton and an electron in the ${}^3\text{MLCT}$ excited state, but until now such excited-state BDFEs had not been reported. Based on published acidity constants and redox potentials we have tried to estimate some excited-state BDFEs for previously investigated complexes (Table 3), but these data should be considered with caution because often different solvents were used for determination of pK_a values and redox potentials, and there are

considerable uncertainties in their excited-state energies. The general observation is that excited-state BDFEs are in the range between 30 and 50 kcal mol⁻¹. As noted before and as evident from eq. 1, the changes in redox potential have a more important influence on the BDFE than changes of the acidity constants.^[52]

Conclusions

All relevant thermodynamic parameters regarding proton-coupled oxidation, i. e., formal H-atom donation, were determined for three photoactive complexes in 1:1 (v:v) $\text{CH}_3\text{CN} / \text{H}_2\text{O}$. The key findings are: (i) Deprotonation of the studied complexes yields a gain in reducing power of 0.3 V in the ground state and 0.1 – 0.2 eV in the emissive excited state. (ii) the formal N-H BDFE can be tuned over a range of ca. 20 kcal mol⁻¹ by varying the spectator ligands; (iii) formal H atom release is facilitated by roughly 50 kcal mol⁻¹ upon excitation of these complexes to their long-lived ${}^3\text{MLCT}$ excited states, reaching excited state BDFEs down to 34 kcal mol⁻¹. Thus, the photo-excited $[\text{Ru}^{\text{R}}\text{pyimH}]^{2+}$ complexes are very strong formal H-atom donors even when compared to metal-hydride complexes which are used as hydrogenation catalysts.

Experimental Section

Methods and Equipment

All commercially available chemicals for synthesis were used as received. Acetonitrile for electrochemical and photophysical measurements was HPLC grade, and water had Millipore standard. Salts for buffers were used as received, and aqueous buffer solutions (0.1 M concentration) were prepared according to reported procedures.^[59] The following buffers were used for the various pH ranges: TsOH / TsONa (pH 1.0-2.0), citric acid (pH 2.2-3.6), glycine / HCl (pH 2.2-3.6) acetate (pH 3.6-5.6), phosphate (pH 5.8-8.0), glycine / NaOH (pH 8.6-10.6), phosphate (pH 11.0-12.0). Unless otherwise noted, all measurements were performed in 1:1 (v:v) $\text{CH}_3\text{CN} / \text{H}_2\text{O}$ with a final buffer concentration of 0.05 M at 25 °C. The pH of the solvent mixture was determined by correcting the measured pH value (pH^{meas}) in the mixture by using the relationship $\text{pH} = \text{pH}^{\text{meas}} - \delta$. For the 1:1 (v:v) $\text{CH}_3\text{CN} / \text{H}_2\text{O}$ mixture, the correction constant δ is -0.257.^[60] All

pH values reported in this publication were corrected accordingly, and pK_a values that were taken from reference^[41] were also corrected accordingly. ¹H NMR spectra were measured on a 400 MHz Bruker Avance III instrument. UV-Vis spectra were measured on a Cary 5000 instrument from Varian. Cyclic voltammetry was performed on a Versastat3-200 potentiostat from Princeton Applied Research using a glassy carbon disk working electrode, a saturated calomel electrode as reference electrode, and a platinum wire was used as counter electrode, 0.05 M buffer served as supporting electrolyte. Prior to voltage sweeps at rates of 0.1 V s⁻¹, the solutions were flushed with argon. For reversible cyclic voltammograms the average of reductive and oxidative peak potentials was used to determine the redox potential; for irreversible oxidations, the inflection point of the oxidative sweep was used as an approximation for the oxidation potential. Steady-state luminescence experiments were performed on a Fluorolog-3 apparatus from Horiba Jobin-Yvon. Samples were excited at wavelengths corresponding to the isosbestic points observed in acid-base titration experiments in **Fehler! Verweisquelle konnte nicht gefunden werden.** and **Fehler! Verweisquelle konnte nicht gefunden werden.** of the Supporting Information. Luminescence lifetime and transient absorption experiments occurred on an LP920-KS spectrometer from Edinburgh Instruments equipped with an iCCD detector from Andor. The excitation source was the frequency-doubled output from a Quantel Brilliant b laser. For aerated optical spectroscopic experiments, quartz cuvettes from Starna and Helma were used. For all deaerated optical spectroscopic experiments the samples were de-oxygenated via three subsequent freeze-pump-thaw cycles in home-built quartz cuvettes that were specifically designed for this purpose.

Synthetic Procedures

[Ru(^tBu)₂bpy)₂pyimH](PF₆)₂ ([Ru^tBu₂pyimH](PF₆)₂): The following procedure was applied based on a previously published protocol.^[41] [Ru(^tBu)₂bpy)₂Cl₂] (177 mg, 250 μmol, 1.00 eq.) was suspended at reflux in a degassed mixture of water (5 mL) and EtOH (5 mL). 2-(1H-imidazol-2-yl)pyridine (44.0 mg, 305 μmol, 1.22 eq.) was added and the reaction mixture was heated to reflux for 3 h. After cooling to room temperature, a few drops of concentrated aq. HCl were added, and then ethanol was removed in vacuo. After addition of sat. aq. KPF₆ solution the precipitate was filtered, washed with water and Et₂O. The solid was collected yielding the product as an orange solid (193 mg, 180 μmol, 72 %). ¹H-NMR (300 MHz, CDCl₃) δ = 11.76 (s, 1H), 8.30–8.10 (m, 6H), 7.80 (td, J = 7.8, 1.4 Hz, 1H), 7.73 (d, J = 6.0 Hz, 1H), 7.69–7.57 (m, 4H), 7.49 (dd, J = 6.1, 2.0 Hz, 1H), 7.46–7.37 (m, 3H), 7.32 (ddd, J = 7.3, 5.7, 1.3 Hz, 1H), 7.25 (s, 1H), 6.43 (s, 1H), 1.41 (d, J = 6.3 Hz, 36H). C₄₄H₅₅F₁₂N₇P₂Ru: calcd. C, 49.32; H, 5.17; N, 9.14; found: C, 49.32; H, 4.95; N, 9.01. ESI-HRMS: (m/z) calcd. for C₇₈H₆₇N₉O₄Ru²⁺: 391.6782; found: 391.6777.

[Ru(NMe₂)₂bpy)₂pyimH](PF₆)₂ ([Ru^{NMe₂}pyimH](PF₆)₂): The following procedure was applied based on a previously published protocol.^[40] A degassed mixture of [Ru(NMe₂)₂bpy)₂Cl₂] · 4 H₂O (100 mg, 131 μmol, 1.00 eq.), 2-(1H-imidazol-2-yl)pyridine (74.0 mg, 510 μmol, 3.89 eq.) and NEt₃ (0.2 mL) in water (5 mL) and EtOH (5 mL) was heated to reflux for 7 h. After cooling to room temperature, sat. aq. NH₄PF₆ solution (0.5 mL) was added. Some solvent was evaporated in vacuo and the precipitate was filtered and washed with water. The obtained solid was purified by column chromatography (SiO₂, acetone → acetone : H₂O : sat. aq. KNO₃ 100:10:1). The solvent of the red-colored phase was removed in vacuo, 0.1 M acetate buffer (pH 5, 10 mL) and sat. aq. KPF₆ solution were added one after another. The organic solvent was removed in vacuo and the precipitate was collected by filtration. The product was obtained as a red solid (65 mg, 63.7 μmol, 48 %). ¹H-NMR (400 MHz, CD₃CN) δ = 11.80 (s, 1H), 8.03 (d, J = 7.9 Hz, 1H), 7.86 (t, J = 7.7 Hz, 1H), 7.79 (d, J = 5.6 Hz, 1H), 7.47 (d, J = 7.3 Hz, 4H), 7.39 (s, 1H), 7.28 (d, J = 6.5 Hz, 2H), 7.18 (m, 3H), 6.62–6.41 (m, 5H), 3.10 (m, 24H). C₃₆H₄₃F₁₂N₁₁P₂Ru·0.75

CH₃COCH₃·2.5 H₂O: calcd. C, 41.41; H, 4.77; N, 13.89; found C, 41.45; H, 4.78; N, 13.91. ESI-HRMS: (m/z) calcd. for C₃₆H₄₃F₁₂N₁₁P₂Ru²⁺: 365.6368; found: 365.6371.

Acknowledgements

We thank Martin Kuss-Petermann for the synthesis of [Ru^tBu₂pyimH](PF₆)₂. This work was supported by the Swiss National Science Foundation through grant number 200021_156063/1 and through the NCCR Molecular Systems Engineering.

Keywords: photochemistry, thermochemistry, redox chemistry, substituent effect, ruthenium

- [1] C. R. Bock, T. J. Meyer, D. G. Whitten, *J. Am. Chem. Soc.* **1974**, *96*, 4710–4712.
- [2] R. Bensasson, C. Salet, V. Balzani, *J. Am. Chem. Soc.* **1976**, *98*, 3722–3724.
- [3] C. K. Prier, D. A. Rankic, D. W. C. MacMillan, *Chem. Rev.* **2013**, *113*, 5322–5363.
- [4] H. Huo, X. Shen, C. Wang, L. Zhang, P. Röse, L.-A. Chen, K. Harms, M. Marsch, G. Hilt, E. Meggers, *Nature* **2014**, *515*, 100–103.
- [5] L. A. Büldt, X. Guo, A. Prescimone, O. S. Wenger, *Angew. Chem., Int. Ed.* **2016**, *55*, 11247–11250.
- [6] S. Berardi, S. Drouet, L. Francàs, C. Gimbert-Suriñach, M. Guttentag, C. Richmond, T. Stoll, A. Llobet, *Chem. Soc. Rev.* **2014**, *43*, 7501–7519.
- [7] L. Hammarström, *Acc. Chem. Res.* **2015**, *48*, 840–850.
- [8] J. L. Fillol, Z. Codolà, I. Garcia-Bosch, L. Gómez, J. J. Pla, M. Costas, *Nat. Chem.* **2011**, *3*, 807–813.
- [9] C. J. Gagliardi, B. C. Westlake, C. A. Kent, J. J. Paul, J. M. Papanikolas, T. J. Meyer, *Coord. Chem. Rev.* **2010**, *254*, 2459–2471.
- [10] E. C. Gentry, R. R. Knowles, *Acc. Chem. Res.* **2016**, *49*, 1546–1556.
- [11] K. T. Tarantino, P. Liu, R. R. Knowles, *J. Am. Chem. Soc.* **2013**, *135*, 10022–10025.
- [12] M. Zhang, T. Irebo, O. Johansson, L. Hammarström, *J. Am. Chem. Soc.* **2011**, *133*, 13224–13227.
- [13] O. S. Wenger, *Acc. Chem. Res.* **2013**, *46*, 1517–1526.
- [14] M. Sjödin, S. Styring, H. Wolpher, Y. Xu, L. Sun, L. Hammarström, *J. Am. Chem. Soc.* **2005**, *127*, 3855–3863.
- [15] M. Sjödin, S. Styring, B. Åkermark, L. Sun, L. Hammarström, *J. Am. Chem. Soc.* **2000**, *122*, 3932–3936.
- [16] A. Magnuson, H. Berglund, P. Korall, L. Hammarström, B. Åkermark, S. Styring, L. Sun, *J. Am. Chem. Soc.* **1997**, *119*, 10720–10725.
- [17] P. Dongare, S. Maji, L. Hammarström, *J. Am. Chem. Soc.* **2016**, *138*, 2194–2199.
- [18] G. F. Manbeck, E. Fujita, J. J. Concepcion, *J. Am. Chem. Soc.* **2016**, *138*, 11536–11549.
- [19] J. Chen, M. Kuss-Petermann, O. S. Wenger, *J. Phys. Chem. B*

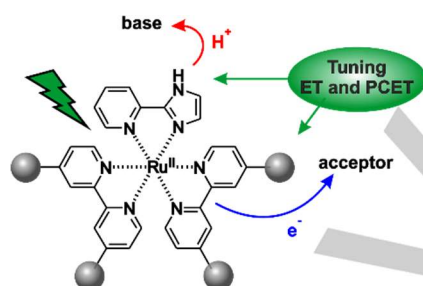
- 2015, 119, 2263–2273.
- [20] H. G. Yayla, R. Knowles, *Synlett* **2014**, 25, 2819–2826.
- [21] J. Nomrowski, O. S. Wenger, *Inorg. Chem.* **2015**, 54, 3680–3687.
- [22] T. T. Eisenhart, J. L. Dempsey, *J. Am. Chem. Soc.* **2014**, 136, 12221–12224.
- [23] B. C. Westlake, M. K. Brennaman, J. J. Concepcion, J. J. Paul, S. E. Bettis, S. D. Hampton, S. A. Miller, N. V. Lebedeva, M. D. Forbes, A. M. Moran, et al., *Proc. Natl. Acad. Sci. U. S. A.* **2011**, 108, 8554–8558.
- [24] O. S. Wenger, *Coord. Chem. Rev.* **2015**, 282–283, 150–158.
- [25] J. C. Freys, G. Bernardinelli, O. S. Wenger, *Chem. Comm.* **2008**, 4267–4269.
- [26] C. Bronner, O. S. Wenger, *Inorg. Chem.* **2012**, 51, 8275–8283.
- [27] A. Pannwitz, O. S. Wenger, *Phys. Chem. Chem. Phys.* **2016**, 18, 11374–11382.
- [28] C. Bronner, O. S. Wenger, *J. Phys. Chem. Lett.* **2012**, 3, 70–74.
- [29] S. M. Barrett, C. L. Pitman, A. G. Walden, A. J. M. Miller, *J. Am. Chem. Soc.* **2014**, 136, 14718–14721.
- [30] D. R. Weinberg, C. J. Gagliardi, J. F. Hull, C. F. Murphy, C. A. Kent, B. C. Westlake, A. Paul, D. H. Ess, D. Granville, T. J. Meyer, *Chem. Rev.* **2012**, 112, 4016–4093.
- [31] J. J. Concepcion, M. K. Brennaman, J. R. Deyton, N. V. Lebedeva, M. D. E. Forbes, J. M. Papanikolas, T. J. Meyer, *J. Am. Chem. Soc.* **2007**, 129, 6968–6969.
- [32] N. V. Lebedeva, R. D. Schmidt, J. J. Concepcion, M. K. Brennaman, I. N. Stanton, M. J. Therien, T. J. Meyer, M. D. E. Forbes, *J. Phys. Chem. A* **2011**, 115, 3346–3356.
- [33] M.-A. Haga, *Inorg. Chim. Acta* **1983**, 75, 29–35.
- [34] K. M. Lancaster, J. B. Gerken, A. C. Durrell, J. H. Palmer, H. B. Gray, *Coord. Chem. Rev.* **2010**, 254, 1803–1811.
- [35] J. J. Warren, T. A. Tronic, J. M. Mayer, *Chem. Rev.* **2010**, 110, 6961–7001.
- [36] C. R. Waidmann, A. J. M. Miller, C.-W. A. Ng, M. L. Scheuermann, T. R. Porter, T. A. Tronic, J. M. Mayer, *Energy Environ. Sci.* **2012**, 5, 7771–7780.
- [37] J. Choi, M. E. Pulling, D. M. Smith, J. R. Norton, *J. Am. Chem. Soc.* **2008**, 130, 4250–4252.
- [38] E. F. Van Der Eide, M. L. Helm, E. D. Walter, R. M. Bullock, *Inorg. Chem.* **2013**, 52, 1591–1603.
- [39] S. Anderson, E. C. Constable, K. R. Seddon, J. E. Turp, J. E. Baggott, M. J. Pilling, *J. Chem. Soc., Dalton Trans.* **1985**, 2247–2261.
- [40] S. J. Slattery, N. Gokaldas, T. Mick, K. A. Goldsby, *Inorg. Chem.* **1994**, 33, 3621–3624.
- [41] R. Hönes, M. Kuss-Petermann, O. S. Wenger, *Photochem. Photobiol. Sci.* **2013**, 12, 254–261.
- [42] T. Ben Hadda, H. Le Bozec, *Polyhedron* **1988**, 7, 575–577.
- [43] R. F. Carina, L. Verzegnassi, G. Bernardinelli, A. F. Williams, *Chem. Comm.* **1998**, 2681–2682.
- [44] H. Jones, M. Newell, C. Metcalfe, S. E. Spey, H. Adams, J. A. Thomas, *Inorg. Chem. Commun.* **2001**, 4, 475–477.
- [45] M. J. Fuentes, R. J. Bognanno, W. G. Dougherty, W. J. Boyko, W. Scott Kassel, T. J. Dudley, J. J. Paul, *Dalt. Trans.* **2012**, 41, 12514–12523.
- [46] S. Klein, W. G. Dougherty, W. S. Kassel, T. J. Dudley, J. J. Paul, *Inorg. Chem.* **2011**, 50, 2754–2763.
- [47] L. M. Tolbert, K. M. Soltsev, *Acc. Chem. Res.* **2002**, 35, 19–27.
- [48] R. M. O'Donnell, R. N. Sampaio, G. Li, P. G. Johansson, C. L. Ward, G. J. Meyer, *J. Am. Chem. Soc.* **2016**, 138, 3891–3903.
- [49] F. G. Bordwell, X. Zhang, J. P. Cheng, *J. Org. Chem.* **1991**, 56, 3216–3219.
- [50] F. G. Bordwell, X. M. Zhang, J. P. Cheng, *J. Org. Chem.* **1993**, 58, 6410–6416.
- [51] M. Bourrez, R. Steinmetz, S. Ott, F. Gloaguen, L. Hammarström, *Nat. Chem.* **2015**, 7, 140–145.
- [52] A. Wu, J. Masland, R. D. Swartz, W. Kaminsky, J. M. Mayer, *Inorg. Chem.* **2007**, 46, 11190–11201.
- [53] A. M. Bond, M. Haga, *Inorg. Chem.* **1986**, 25, 4507–4514.
- [54] D. P. Rillema, R. Sahai, P. Matthews, A. K. Edwards, R. J. Shaver, L. Morgan, *Inorg. Chem.* **1990**, 29, 167–175.
- [55] A. Wu, J. M. Mayer, *J. Am. Chem. Soc.* **2008**, 130, 14745–14754.
- [56] S. M. Zakeeruddin, D. M. Fraser, N. M.-K., M. Grätzel, *J. Electroanal. Chem.* **1992**, 337, 253–283.
- [57] A. A. Vlcek, E. S. Dodsworth, W. J. Pietro, A. B. P. Lever, *Inorg. Chem.* **1995**, 34, 1906–1913.
- [58] A. Juris, V. Balzani, F. Barigelletti, S. Campagna, P. Belser, A. von Zelewsky, *Coord. Chem. Rev.* **1988**, 84, 85–277.
- [59] D. D. Perrin, B. Dempsey, *Buffers for pH and Metal Ion Control*, Chapman And Hall, London, **1979**.
- [60] L. G. Gagliardi, C. B. Castells, C. Ràfols, M. Rosés, E. Bosch, *Anal. Chem.* **2007**, 79, 3180–3187.

Entry for the Table of Contents

Layout 1:

FULL PAPER

A series of ruthenium(II) pyridylimidazole complexes with various substituents on the bipyridine spectator ligands were characterized in the ground and excited state with respect to reducing power and formal bond dissociation free energy (BDFE), applicable for proton-coupled electron transfer (PCET).



PCET Reagents

Andrea Pannwitz, Alessandro Prescimone, and Oliver S. Wenger*

Page No. – Page No.

Ruthenium(II) Pyridylimidazole Complexes as Photoreductants and PCET Reagents